

# Chirality and protein folding

Joanna I Kwiecińska and Marek Cieplak<sup>1</sup>

Institute of Physics, Polish Academy of Sciences, Aleja Lotników 32/46, 02-668 Warsaw, Poland

E-mail: mc@ifpan.edu.pl

Received 5 October 2004, in final form 18 November 2004

Published 22 April 2005

Online at [stacks.iop.org/JPhysCM/17/S1565](http://stacks.iop.org/JPhysCM/17/S1565)

## Abstract

There are several simple criteria of folding to a native state in model proteins. One of them involves crossing of a threshold value of the root mean square deviation distance away from the native state. Another checks whether all native contacts are established, i.e. whether the interacting amino acids come closer than some characteristic distance. We use Go-like models of proteins and show that such simple criteria may prompt one to declare folding even though fragments of the resulting conformations have a wrong sense of chirality. We propose that a better condition of folding should augment the simple criteria with the requirement that most of the local values of the chirality should be nearly native. The kinetic discrepancy between the simple and compound criteria can be substantially reduced in the Go-like models by providing the Hamiltonian with a term which favours native values of the local chirality. We study the effects of this term as a function of its amplitude and compare it to other models such as ones with side groups and ones with angle-dependent potentials.

## 1. Introduction

Theoretical studies of the kinetics of protein folding in off-lattice models encounter a difficulty when it comes to making a decision about at what stage of the temporal evolution from an unfolded state the system can be considered as having reached the native conformation. The native conformation is usually known within some experimental resolution but, in models, this is a state of ‘zero measure’ in the three-dimensional space. Criteria of folding must then involve some finite effective spatial extension of the native conformation and then checking whether an evolving conformation has already entered the resulting native ‘cocoon’. An example of providing a way to define such a cocoon is given in [1–4] where one studies features in time evolution of distortions in shape of the native conformation. The shape distortion method, however, turned out to be rather subtle and applicable, in practice, only to secondary structures of proteins.

<sup>1</sup> Author to whom any correspondence should be addressed.

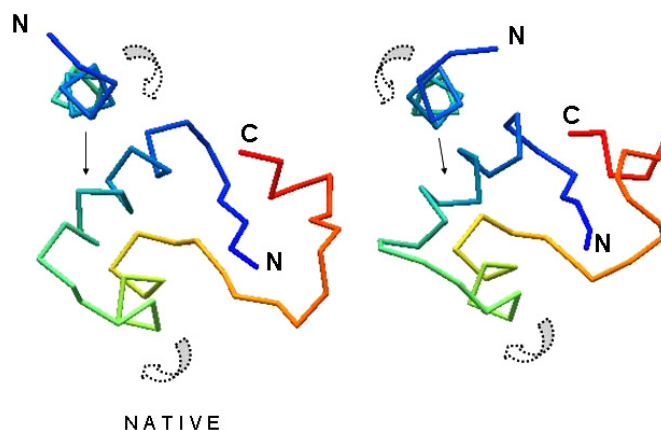


**Figure 1.** Conformations of crambin in the backbone representation (there are 46 residues in crambin). The figure on the left-hand side shows the native structure (1crn in the Protein Data Bank). The figure on the right-hand side corresponds to the conformation in which all native contacts are established through a folding process accomplished through a molecular dynamics evolution in the Go-like model that is used in this paper. Even though all amino acids are within the contact establishing distances from each other in the folded state, some local chiralities are opposite to what they should be. The sense of chirality is shown by the spinning arrows. The helical structure placed at the top of the figure winds in opposite senses in the two panels.

(This figure is in colour only in the electronic version)

Simple and widely used criteria of folding postulate the existence of a variable that crosses a predefined threshold value on folding. One example of such a variable is the root mean square deviation (RMSD) distance away from the native state. Another is the fraction,  $Q$ , of the established native contacts which implies descending below some selected value of the total energy. Usually, the threshold value of  $Q$  is selected to be equal to 1. Note, however, that the very notion of an established contact itself depends on two amino acids coming closer together than some threshold value,  $r_c$ , of their mutual distance. In the following, the folding criterion based on the RMSD distance will be denoted by  $R$  and the criterion based on contacts by  $Q$ . For completeness, we also consider a third criterion, denoted by  $A$ , which is based on the angular properties of the protein backbone. Criterion  $A$  involves checking whether the bond and dihedral angles are at their native values within a chosen range.

In this paper, we use coarse-grained Go-like models of proteins [5, 6] with the Lennard-Jones potentials in the contacts. We show that all three of these simple criteria may prompt one to declare folding even though fragments of the resulting conformations have a non-native sense of chirality—a point that has already been noted by Ortiz *et al* [7]. Figure 1, for crambin, shows an example of this problem when the  $Q$  criterion is used. It is seen that the folding process may generate a left-handed  $\alpha$ -helix instead of the right-handed one that is actually present in the true native conformation. This misfolding event occurs despite the fact that all native contacts are found to be within their respective values of  $r_c$  (1.5 times the characteristic length parameter  $\sigma$  in the potential) and the RMSD distance away from the native state is only around 2.5 Å. In order to counter this difficulty with the folding criteria one may consider adopting more stringent values of the threshold parameters but this approach turns out to be impractical for it usually leads to prohibitively long time evolution, i.e. it results in a lack of folding. Even though our conclusions are drawn from studies of Go-like models, we expect similar problems also to be encountered in all-atom simulations.

We propose that a reasonable condition of folding should combine the simple criteria with the requirement that all local values of the chirality should be nearly native. We show that setting of the local chiralities to native-like values may or may not precede the ‘calls’ resulting from the simple criteria, depending on the criterion and the type of a protein, but the compound requirement allows for more accurate studies of folding and typically generates structures that appear to be of correct topology.

The kinetic discrepancy between the simple and compound criteria can be substantially reduced in the Go-like models by providing the Hamiltonian with an extra term which favours native values of the local chirality as introduced in [8]. We study the effects of this term as a function of its amplitude and select a value of it that could be used in simulations.

As will be made explicit later, the definition of the local chirality involves coordinates of four subsequent  $C^\alpha$  atoms. It should be noted that a definition of the bond angle involves three  $C^\alpha$  atoms and that of the dihedral angle, four. One may ask then two questions: First, how does the chirality based criterion relate to the criterion involving the bond and dihedral angles? Second, is it better to use potentials that favour the native sense of chirality or those which favour the native values of the bond and dihedral angles? We discuss these issues at the end of the paper and find the chirality potential to act in a comparable way to the angular potential. However, its usage is much more economical in simulations. We also find that simple modelling of the side groups by the  $C^\beta$  atoms does not automatically take care of making the chirality in the folded state correct.

## 2. The Go-like model

We perform molecular dynamics simulations of a continuum space coarse-grained Go-like model. The Go-like models are defined through experimentally determined native conformations of proteins as stored in the Protein Data Bank [9]. The details of our approach are described in [3, 4]. Each amino acid is represented by a point particle of mass  $m$  located at the position of the  $C^\alpha$  atom. The interactions between amino acids are divided into native and non-native contacts. We determine the native contacts by considering the all-atom native structure and by identifying those pairs of amino acids in which there is an overlap between effective spheres that are associated with heavy atoms [8, 10]. These spheres have radii that are a factor of 1.24 larger than the atomic van der Waals radii [11] to account for the softness of the potential. The native contacts are then represented by the Lennard-Jones potentials  $4\epsilon[(\sigma_{ij}/r_{ij})^{12} - (\sigma_{ij}/r_{ij})^6]$ , where  $r_{ij} = |\vec{r}_i - \vec{r}_j|$  is the distance between  $C^\alpha$  atoms  $i$  and  $j$  located at  $\vec{r}_i$  and  $\vec{r}_j$  respectively. The length parameters  $\sigma_{ij}$  are determined such that the minimum of the pair potential coincides with the distance between  $C^\alpha$  atoms in the native structure. In order to prevent entanglements, the remaining pairwise interactions, i.e. the non-native contacts, correspond to a pure repulsion. This is accomplished by taking the Lennard-Jones potential with  $\sigma_{ij} = \sigma = 5 \text{ \AA}$  and truncating it at  $2^{1/6}\sigma$ .

All contacts have the same energy scale  $\epsilon$ . This energy scale corresponds to between 800 and 2300 K as it effectively represents hydrogen bond and hydrophobic interactions. The room temperature should then correspond to values of  $\tilde{T} = k_B T/\epsilon$  of about 0.1–0.3 ( $k_B$  is the Boltzmann constant). Neighbouring  $C^\alpha$  atoms are tethered by a harmonic potential with a minimum at 3.8  $\text{\AA}$  and the force constant of  $100\epsilon \text{ \AA}^{-2}$ .

The equations of motion are integrated using a fifth-order predictor–corrector algorithm with time step  $dt = 0.005\tau$ . A Langevin thermostat with damping constant  $\gamma$  is coupled to each  $C^\alpha$  to control the temperature. For the results presented below,  $\gamma = 2m/\tau$ , where  $\tau = \sqrt{m\sigma^2/\epsilon} \sim 3 \text{ ps}$  is the characteristic time for the Lennard-Jones potential. This produces the overdamped dynamics appropriate for proteins in a solvent [8], but is roughly 25 times

smaller than the realistic damping from water [12]. Tests with larger  $\gamma$  confirm a linear scaling of folding times with  $\gamma$  [3, 4]. So the folding times reported below should be multiplied by 25 for a more meaningful comparison to experiment.

The folding processes are characterized by the order in which native contacts are formed. At a finite  $T$ , a pair distance  $r_{ij}$  may fluctuate around a selected cut-off value. Thus, when discussing folding using the contact criterion, we determine the average time  $t_c$  for each contact to form for the first time. Unless stated otherwise, as the cut-off value for the presence of a contact between amino acids  $i$  and  $j$  we take  $1.5\sigma_{ij}$  in model proteins and  $1.36\sigma_{ij}$  in model secondary structures. The latter value is equal to the inflection distance for the Lennard-Jones potential. This choice of the prefactor does not matter much for the secondary structures but choosing the inflection distance for proteins makes the folding process prohibitively long lasting. Note that the cut-off  $r_c$  depends on the pair of amino acids in our model.

The chirality of residue  $i$  is defined as

$$C_i = \frac{(\vec{v}_{i-1} \times \vec{v}_i) \cdot \vec{v}_{i+1}}{d_0^3}, \quad (1)$$

where  $\vec{v}_i = \vec{r}_{i+1} - \vec{r}_i$ , and  $d_0 = |v_i|$  is a distance between neighbouring residues as represented by the  $C^\alpha$  atoms. For a protein of  $N$  amino acids,  $C_i$  is defined for  $i$  from 2 to  $N - 2$ . In equation (1), the amino acids are labelled from the terminal  $N$  to the terminal  $C$ . It is possible to consider an alternative definition which would involve proceeding in the opposite way and which would define chiralities for  $i$  from 3 to  $N - 1$ . Another possibility is to consider a symmetrized combination of the two definitions. We have found, however, that these alternative variants work quite similarly to the basic definition.

In the unlikely event in which all of the atoms involved in the determination of  $C_i$  are located in a plane, one gets a  $C_i$  which is equal to zero. Otherwise  $C_i$  is positive or negative for the right-handed and left-handed local turns respectively. The magnitudes are small in nearly planar loop regions. The distribution of  $C_i$  in proteins is essentially bimodal [8]. A maximum around 0.7 corresponds to  $\alpha$ -helices. We will show that in  $\beta$ -sheets,  $C_i$  ranges between  $-0.15$  and  $0.15$ . In turns and loops,  $C_i$  can also be either positive or negative.

We illustrate the findings of our studies by focusing on the (16–31) helical fragment of the P chain of the capsid protein P24—1e6j, the (41–56) hairpin of the protein 1pga and on crambin, 1crn. The folding times were determined as the median first passage time. 501 different trajectories were used in the case of secondary structures and at least 101 trajectories in the case of crambin.

### 3. Criteria of folding

Consider 1e6j(16–31)—the helical fragment of 16 monomers. Figure 2 shows examples of conformations that are declared folded according the criteria  $Q$ ,  $R$ , and  $A$ . The first two criteria were specified in the introduction. As to the  $A$  criterion, we require that the local bond,  $\theta_i$ , and dihedral,  $\phi_i$ , angles are within  $\pm\Delta\theta$  and  $\pm\Delta\phi$  of the native values respectively. We take rather generous  $\Delta\theta$  and  $\Delta\phi$  of  $60^\circ$  in order to get folding times which are comparable to those obtained through the other two criteria. Values which are substantially more stringent usually yield no folding in computationally accessible time.

It is seen that each of the dynamically obtained example conformations has regions, usually at the terminals, which twist in the opposite sense relative to what is found in the native conformation. This misfolding phenomenon is captured by the values of the local chiralities that are listed in the caption of figure 2.

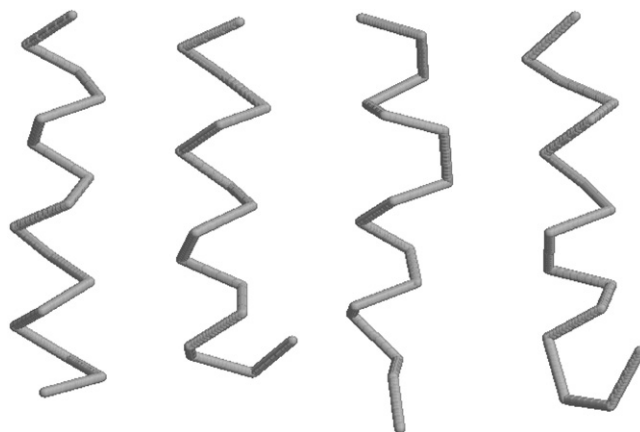


**Figure 2.** Backbone conformations of the  $\alpha$ -helix 1e6j(16–31), extracted from the protein 1e6j. The first conformation shown is native. The remaining conformations are shown at a stage when folding is considered to be accomplished. The time evolution is performed as the molecular dynamics process in the Go-like model. The starting conformation corresponds to a straight line. The folding criteria are  $Q$ ,  $R$ , and  $A$ , left to right, respectively. The values of the local chiralities for  $i$  running from the second to the second from the end terminal amino acid are as follows. As found in the true native state: 0.83, 0.71, 0.75, 0.78, 0.81, 0.84, 0.80, 0.71, 0.81, 0.64, 0.84, 0.36, 0.63. At folding declared by criterion  $Q$ : 0.84, 0.64, 0.82, 0.76, 0.71, 0.81, 0.64, 0.76, 0.74, 0.79, 0.46, 0.60,  $-0.50$ . At folding declared by criterion  $R$ :  $-0.79$ ,  $-0.77$ ,  $-0.55$ ,  $-0.77$ ,  $-0.48$ , 0.66, 0.60, 0.79, 0.79, 0.59, 0.91, 0.37, 0.34. At folding declared by criterion  $A$ : 0.88, 0.45, 0.75, 0.69, 0.86, 0.87, 0.91, 0.66, 0.84, 0.66, 0.86, 0.39,  $-0.18$ .

One way to characterize this phenomenon is to count the number,  $b$ , of  $C_i$ s that have a sign which is opposite to the native sign. The distributions of  $b$  for the helix and for the (41–56) hairpin fragment of the protein 1pga are shown in the top panels of figure 3. The zero value of  $b$  means the absence of chirality defects. It is seen that the distributions depend on the folding criterion used and  $A$  is found to be the most successful in this respect:  $b$  is concentrated at values not exceeding 3. The  $Q$  and  $R$  criteria work in a comparable way for the hairpin, but  $Q$  is worse for the helix (for several other helices it was found to be comparable). The bottom panels of figure 3 illustrate the sequential distribution of the local chirality defects,  $b_i$ . ( $i$  is counted here from the beginning of the fragment and not from the  $N$  terminal of the host protein.) In the helix, the three criteria generate defects throughout the chain, though, for this particular helix,  $A$  favours defects arising closer to the  $C$  terminal. On the other hand, the defects generated in the hairpin as a result of adopting the  $A$  criterion are localized at the centre (and do not depend on the example of a hairpin). The other two criteria favour no particular region in the hairpin.

In order to monitor the chirality defects dynamically we introduce the parameter  $K$  which compares the values of  $C_i$  to the native values,  $C_i^{\text{NAT}}$ , and counts the values which can be considered as being substantially native-like, i.e. which are of the right sign and have magnitudes at least 50% of the native strength. A convenient definition of  $K$  is then given by

$$K = \sum_{i=2}^{N-2} \Theta(C_i/C_i^{\text{NAT}} - 0.5), \quad (2)$$

where  $\Theta(x)$  is the step function ( $\Theta(x)$  is 1 if  $x \geq 0$  and 0 otherwise).

The top left panel of figure 4 shows that the local values of  $C_i$  may have a rapid temporal evolution which translates into a noisy behaviour of  $K$ . It is thus not realistic to seek the

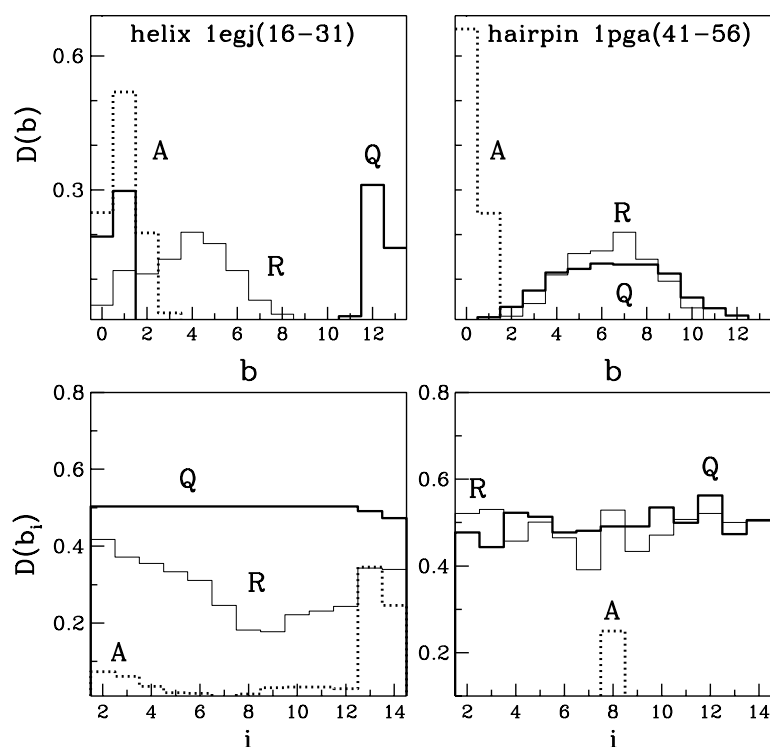


**Figure 3.** The top panels show distributions,  $D(b)$ , of the numbers,  $b$ , of the wrong signed local chiralities when folding is declared according to the criteria  $Q$ ,  $A$ , and  $R$ , as indicated. The left and right panels are for the helix 1ejj(16–31) and the hairpin 1pga(41–56) respectively. The bottom panels show the sequential distribution of such chirality defects.

fully native value  $K_{\text{NAT}}$  of  $N - 3$ . However,  $K_c = 0.75 K_{\text{NAT}}$  is attainable in simulations, as illustrated in the remaining panels of figure 4. These panels show examples of the time evolution of the number of established native contacts,  $N_Q$ , and of  $K$  for two secondary structures and for crambin. In the case of the helix,  $K$  strikes  $K_c$  for the first time in the example trajectory before  $Q$  hits 1 for the first time. The opposite takes place in the illustrative trajectories for crambin and for the hairpin.

We propose that the shape sensitive criterion of folding should combine simple criteria such as  $Q$ ,  $R$ , and  $A$  with a condition on the chirality:

$$K \geq K_c. \quad (3)$$

From now on, we focus on the contact based criterion,  $Q$ . The compound contact–chirality criterion will be denoted by  $Q_K$ . The folding time in the  $Q_K$  criterion is then defined as the first instant when both  $Q = 1$  and  $K \geq K_c$ . Similar conclusions are expected to hold for the  $R$  and  $A$  criteria. The  $Q$  criterion and its extension seem to us to be the simplest to use. When employing the  $R$  criterion an appropriate choice of the cut-off RMSD value ought to involve scaling with the system size as pointed out by Betancourt and Skolnick [13]. We also observe that conditions on the angles are especially hard to satisfy in loop regions.

The compound criterion  $Q_K$  leads, of course, to longer folding times than the simple criterion  $Q$ . This is illustrated in figure 5 which shows three characteristic times,  $t_Q$ ,  $t_K$ , and  $t_{QK}$ , for two secondary structures and for crambin. The first of these times corresponds to the

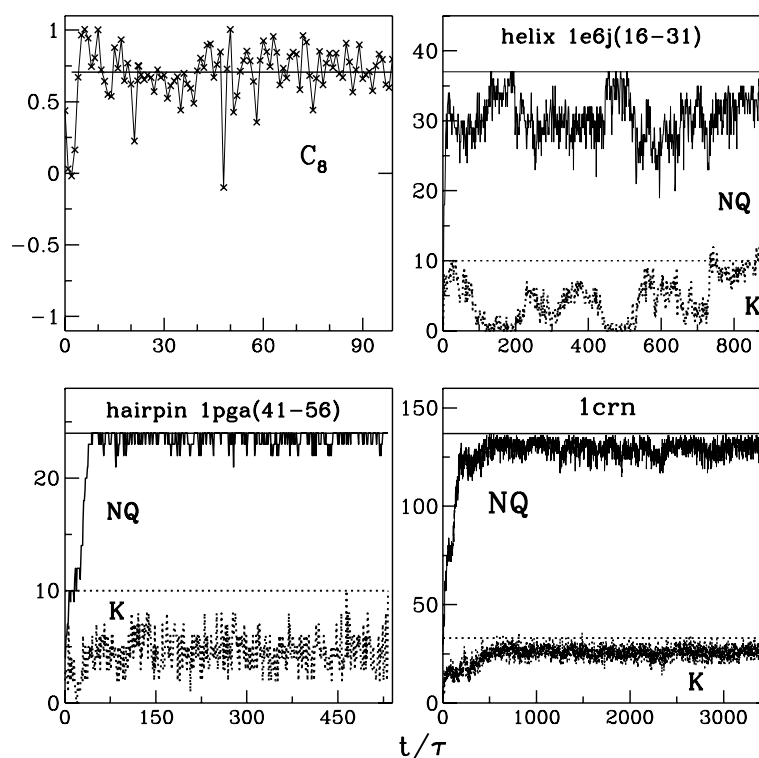


**Figure 4.** The top left panel illustrates the time dependence of the local chirality for a single amino acid—the central amino acid in the 1pga(41–56) hairpin. The remaining panels show examples of the time dependence of the number of established native contacts,  $NQ$ , and the number of established correct chiralities,  $K$ , in single trajectories for the systems indicated. The evolution is stopped when  $Q$  becomes equal to 1 and  $K$  achieves the 75% level of the native value. These target thresholds are indicated by the horizontal lines.

median folding time obtained by using the  $Q$  criterion. The second time denotes the median time for  $K$  to reach  $K_c$  for the first time. Finally,  $t_{QK}$  is the folding time obtained through the compound criterion  $Q_K$ . Both  $t_Q$  and  $t_{QK}$  exhibit the ubiquitous U-shaped dependence on the temperature indicating the presence of the optimal temperature,  $T_{\min}$ , at which folding proceeds the fastest. The value of  $T_{\min}$  itself depends somewhat on the choice of the folding criterion.

At the vicinity of the optimal temperature, the establishment of native-like chirality and that of the native-like number of contacts, separately, are seen to be almost simultaneous for the helix. Establishing both of these quantities simultaneously takes twice as long. In the hairpin, the contacts get established before the chirality. In crambin, there is a clear separation between various stages and the contacts get established first.

The  $Q_K$  criterion leads to a significant reduction in the extension of the wrong chirality defects compared to the  $Q$  criterion. This feature is illustrated in figure 6 for the helix and the hairpin. In the helix, there are no defects with size  $b$  of two or larger (i.e. the left-handed conformations do not arise) and, if present, they are concentrated at the  $C$  terminal where chiralities at the last two sites are not defined. With the simple  $Q$  criterion (figure 3) the defects arise at any site and can extend throughout the helix. The  $Q_K$  criterion also introduces a significant improvement in the conformations found for the hairpin.

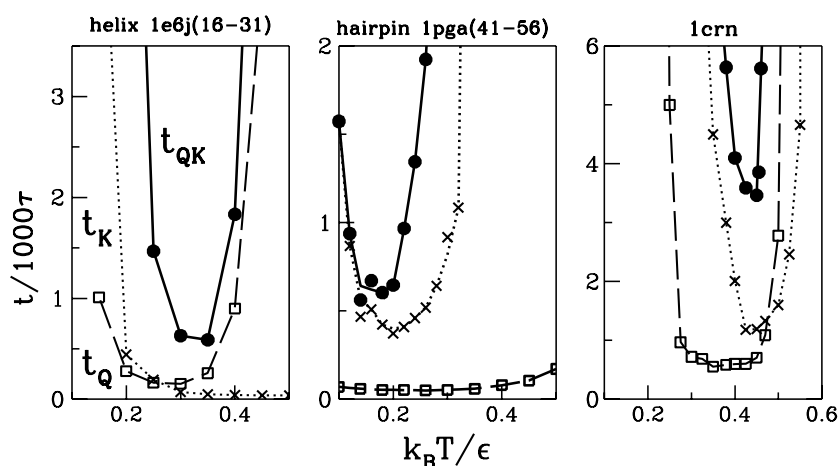


**Figure 5.** The median folding times of the systems indicated at the top of the panels. The data are based on at least 101 trajectories. The dashed curves and the square data points correspond to the contact based folding criterion  $Q$ . The solid curve and the circle data points correspond to the combined contact and chirality based criterion  $QK$ . The dotted curves and the crosses correspond to the times needed to establish 75% of the local chiralities in the native fashion.

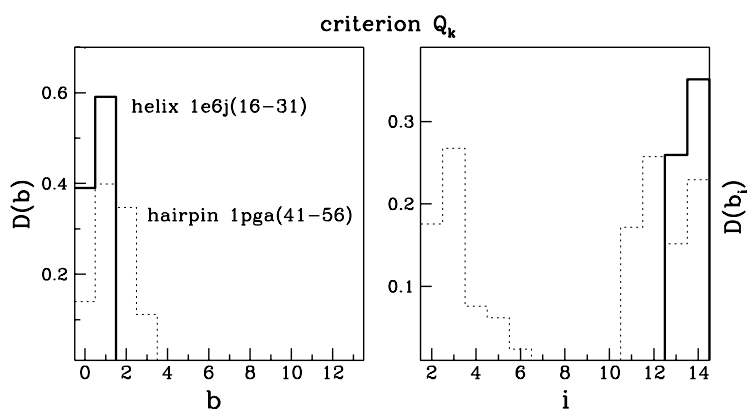


**Figure 6.** The nature of chirality defects in conformations found through the compound criterion  $Q_K$  for the helix (the solid lines) and the hairpin (the dashed lines). The left-hand panel shows the distribution of the sizes of the defects whereas the right-hand panel shows the distribution of their sequential location.

#### 4. The chirality potential

The Go-like modelling works with a potential which favours the native conformation. In this spirit, it seems sensible to improve on the current modelling by adding a potential which favours the native sense of the local chirality. It should also be noted that atomic level interactions in proteins do favour specific senses of chirality that are found in nature. Following [8] (there is a misprint in the definition shown there) we consider the term

$$V^{\text{CHIR}} = \sum_{i=2}^{N-2} \frac{1}{2} \kappa \epsilon C_i^2 \Theta(-C_i C_i^{\text{NAT}}), \quad (4)$$

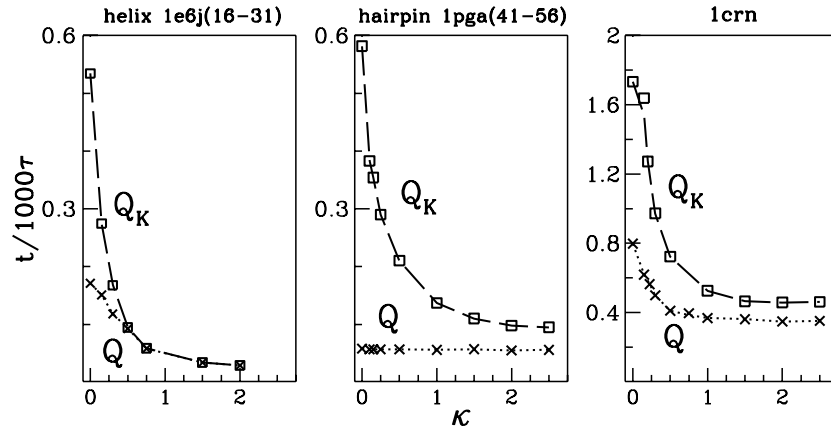


**Figure 7.** Median folding times for the systems indicated at the top of each panel as a function of the strength of the chirality potential. The square data symbols correspond to the  $Q_K$  criterion and the crosses to the  $Q$  criterion. The data points were obtained at  $T_{\min}$  which depends on  $\kappa$  and the criterion.

where the dimensionless parameter  $\kappa$  controls the strength of the potential and its value needs to be selected. The potential  $V^{\text{CHIR}}$  involves a harmonic cost in  $C_i$  if the local chirality is non-native. We have also considered an even more Go-like version of  $V^{\text{CHIR}}$  in which instead of the step function, there is a harmonic penalty for deviations from the native values of the local chiralities:

$$V_1^{\text{CHIR}} = \sum_{i=2}^{N-2} \frac{1}{2} \mu \epsilon (C_i - C_i^{\text{NAT}})^2, \quad (5)$$

where  $\mu$  is a strength parameter. We have found that either choice of the potential leads to qualitatively similar results except that  $V_1^{\text{CHIR}}$  tends to yield broader regions of temperature in which folding is optimal. The results shown in this section are based on equation (4).

Still another way to introduce a chirality-related potential has been recently proposed by Chen *et al* [15] in their studies of homopolypeptides on a lattice. Their definition applies to helices and it involves a linear energy cost (i.e. the chirality acts like an external uniform field and not like a restoring potential). It may be worthwhile to compare the molecular dynamics of such a model with our results.

When one considers not coarse-grained but atomic models then the preference for a native chirality can also be implemented through conditions of consistency with the Ramachandran maps [16, 17] (in this reference the maps are translated into a simplified description of the conformational space).

For a system with the added potential  $V^{\text{CHIR}}$ , the folding times obtained with the criterion  $Q_K$  depend on the value of  $\kappa$ . Figure 7, for the hairpin, shows that the dependence saturates around  $\kappa = 1$ . Furthermore, for  $\kappa \geq 1$  the difference between the folding times obtained with the  $Q$  and  $Q_K$  criteria becomes small. In other words, one can revert to the simple criterion  $Q$  by introducing  $V^{\text{CHIR}}$  with a sufficiently large  $\kappa$ . From now on, we stay with the choice of  $\kappa = 1$  as used in [8] and [14]. The kinetic equivalence of  $Q_K$  to  $Q$  combined with  $V^{\text{CHIR}}$  is qualitative and it appears to be valid in the vicinity of  $T_{\min}$  as shown in figure 8. Away from  $T_{\min}$ ,  $t_Q$  and  $t_{Q_K}$  diverge from each other in the case of the hairpin. For crambin and the helix, there is no divergence. It should be noted, however, that the folding times in systems without  $V^{\text{CHIR}}$  are longer compared to the case of  $\kappa = 1$ , independent of the folding criterion used.

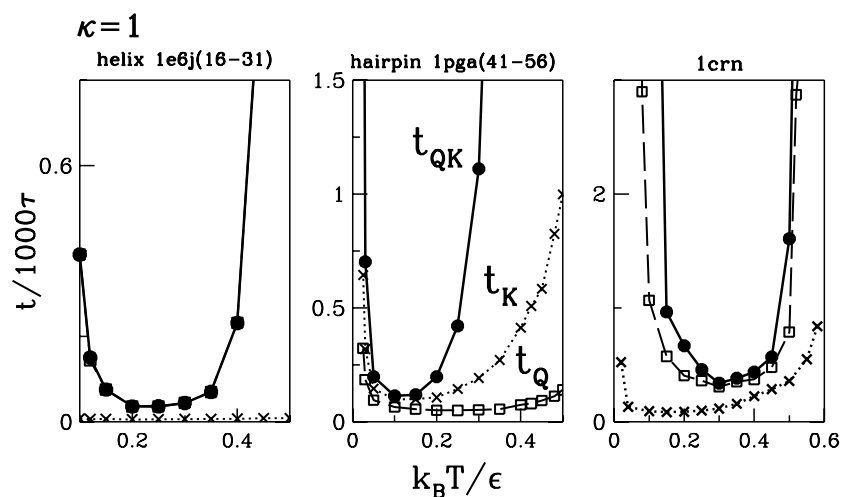


**Figure 8.** The same as figure 5 but with the chiral potential added to the Hamiltonian of the system. For the helix data shown in the left panel,  $t_Q$  and  $t_{Q\kappa}$  coincide within the scale of the figure.

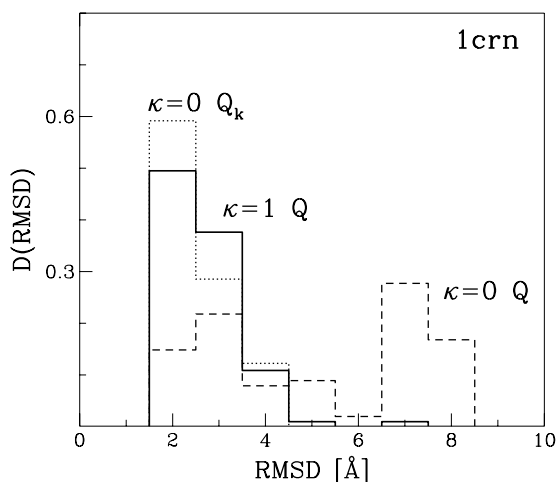


**Figure 9.** The distribution of the RMSD distances away from the native state at folding declared by the criteria indicated. The dashed line corresponds to the Hamiltonian with no chirality potential and the solid line to that with the chirality term with  $\kappa = 1$ . The data are collected at the temperature of optimal folding and are based on 101 trajectories.

The contact criterion  $Q$  with the chiral potential naturally leads to small RMSD values at folding as illustrated in figure 9 for crambin. This figure also shows that the distribution of the RMSD values on folding with the chiral potential and criterion  $Q$  is nearly the same as without the chirality potential but with criterion  $Q_\kappa$ .

One may qualitatively assess the role of the chirality potential on the folding funnel by plotting the free energy as a function of  $Q$ , the fraction of the established native contacts, and  $R$ , the binned values of the RMSD. This  $F(Q, R)$  for the helix is shown in figure 10 at the temperature of optimal folding. It is seen that, in the absence of  $V^{\text{CHIR}}$ , the free energy is endowed with two minima, whereas for  $\kappa = 1$  there is just a simple folding funnel. This indicates that the chirality term leads to a smoother shape of the free energy landscape.

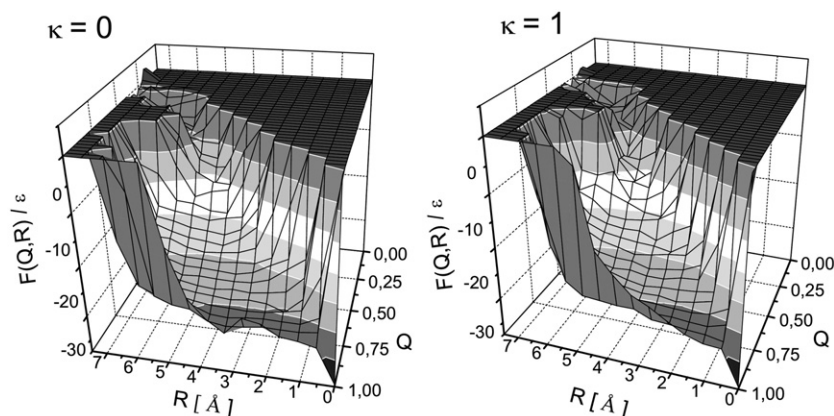


**Figure 10.** The free energy corresponding to specific values of  $Q$  and  $R$  (the RMSD distance away from the native state) for the helix at  $\bar{T} = 0.3$ . The figure on the right-hand side is for the system with the chirality potential with  $\kappa = 1$ . The figure on the left-hand side involves no chirality potential. The results are based on 100 trajectories of 20 000  $\tau$  that start from unfolded conformations.

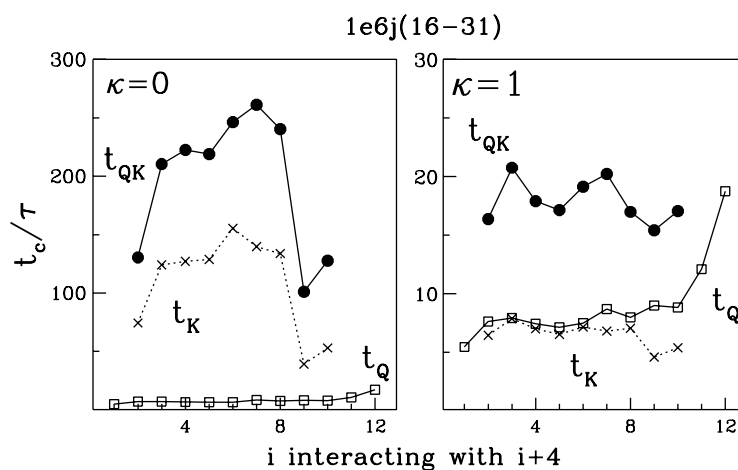


**Figure 11.** The folding scenario for the  $\alpha$ -helix 1e6j(16–31) with (the right panel) and without (the left panel) the chirality potential. The building of the structure is illustrated through the contacts that correspond to the hydrogen bonds—between amino acids  $i$  and  $i + 4$ .  $t_Q$  denotes the average first time for establishing the contact between  $i$  and  $j$  whereas  $t_K$  is the average first time at which the local chiralities of both amino acids are native like.  $t_{QK}$  denotes the average first time at which both the contact and the chiralities are set correctly. The data points are averaged over 2000 trajectories.

We now examine the folding process in more detail by looking at establishment of specific contacts, i.e. by studying the so-called folding scenarios. A contact is said to be established if its amino acids approach each other sufficiently closely—for the first time. A chirality in the contact will be said to be established if both of the amino acids involved acquire native-like chirality (50% of the native value of  $C_i$ ).

The folding scenarios of the helix, hairpin, and crambin are shown in figures 11 to 13 where the case of  $\kappa = 1$  is compared to that of  $\kappa = 0$ . In the case of the helix with  $\kappa = 1$ ,

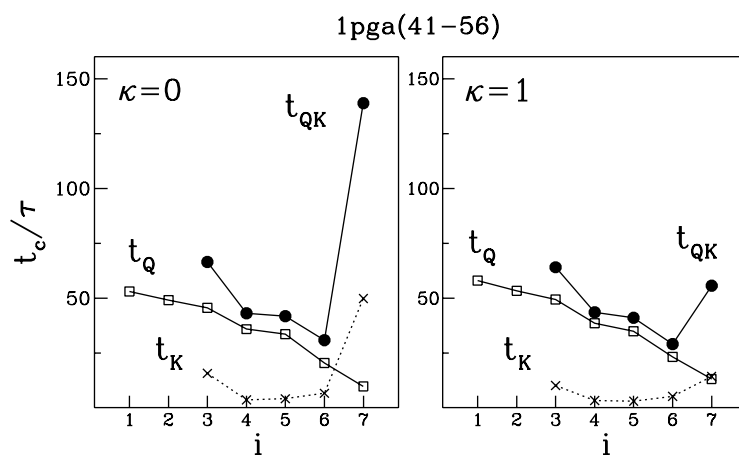


**Figure 12.** Similar to figure 11, but for the hairpin 1pga(41–56). The focus here is on the hydrogen bonds between  $i$  and  $N - i + 1$ .

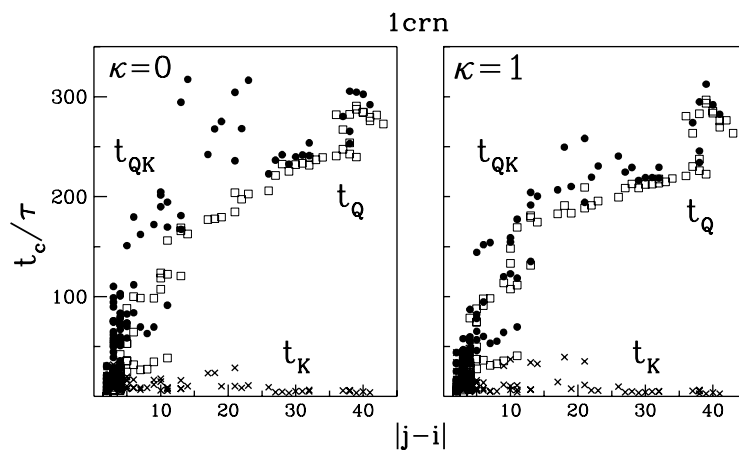


**Figure 13.** The folding scenario of crambin with (the right panel) and without (the left panel) the chirality potential.  $|j - i|$  denotes the sequential distance between two amino acids,  $j$  and  $i$ . The symbols used are as in figure 11.

the average times for establishing pairwise chirality are nearly site independent and practically equal to the times needed to establish the contacts (independently of the establishment of the chirality). The combined criterion essentially doubles the times and leads to somewhat shorter times at the terminals. For  $\kappa = 0$ , there is a stronger preference for initiation at the  $C$  terminal. In the case of the hairpin, there is a tendency to fold the structure from the turn outward, independently of the value of  $\kappa$ , except that it appears to be difficult to establish the right chirality at the turn ( $i = 7$ ). The folding scenario of crambin is nearly monotonic as a function of the contact order. When  $\kappa = 1$ , the folding events as measured by the contact establishment nearly coincide with those determined by the contact–chirality criterion. Thus, in practice, when the chirality potential is present, there is no need for the compound criterion as evidenced also by the distribution of the resulting RMSD (figure 9).

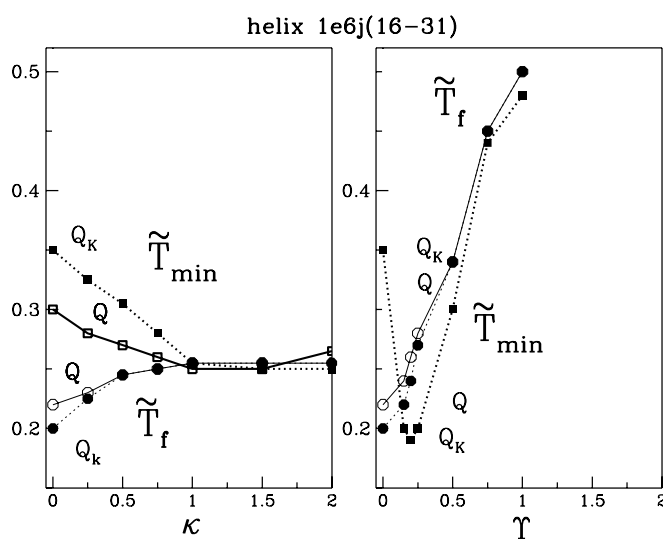


**Figure 14.** The left panel shows the dependence of  $\tilde{T}_{\min}$  and  $T_f$  on the strength of the chirality potential.  $Q$  and  $Q_K$  denote the methods used to define the native basin. The right panel shows similar quantities but as a function of the amplitude of the angle-dependent potential (the values of  $\tilde{T}_{\min}$  do not depend on the material).

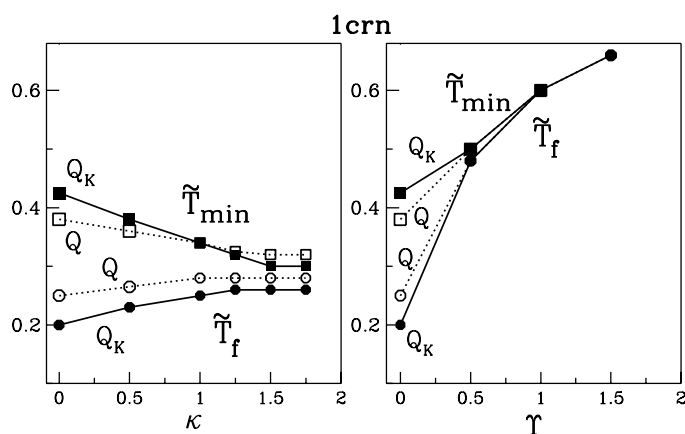


**Figure 15.** Similar to the left hand panel of figure 14, but for crambin.

Finally, we comment on the values of the characteristic temperatures  $T_{\min}$  and  $T_f$ . The latter is the folding temperature at which the probability of staying in the native ‘cocoon’ crosses  $\frac{1}{2}$ .  $T_f$  is a measure of the thermodynamic stability and its determination involves a definition of the cocoon, i.e. whether we use the  $Q$  or  $Q_K$  criterion to define the effective native conformation. The left panel of figure 14 shows that both characteristic temperatures saturate as a function of  $\kappa$  and the results obtained with the two criteria merge. For crambin (figure 15) and the hairpin (not shown) there is no merger but there is a saturation beyond  $\kappa = 1$ .

## 5. The angular potential

We now consider the angle-dependent Go-like potential  $V^{\text{ANG}} = \Upsilon(V^{BA} + V^{DA})$ , where

$$V^{BA} = \sum_{i=1}^{N-2} K_{\theta}(\theta_i - \theta_{0i})^2, \quad (6)$$

and

$$V^{DA} = \sum_{i=1}^{N-3} [K_{\phi}^1(1 + \cos(\phi_i - \phi_{0i})) + K_{\phi}^3(1 + \cos 3(\phi_i - \phi_{0i}))]. \quad (7)$$

Here,  $\theta_i$  and  $\phi_i$  denote the bond and dihedral angles respectively and the subscript 0 indicates the native values that this potential favours. Following Clementi *et al* [18] (see also a further discussion in [19]), we take  $20\epsilon$ ,  $\epsilon$ ,  $0.5\epsilon$  for  $K_{\theta}$ ,  $K_{\phi}^1$ , and  $K_{\phi}^3$  respectively. The quantity  $\Upsilon$  is an overall control parameter of the potential strength such that when  $\Upsilon = 1$  the customarily used strength is obtained [18].

The determination of the dihedral angles involves four sites which suggests a formal similarity to  $V^{\text{CHIR}}$ . We now demonstrate that the effects of the two potentials are different. One example of the difference is shown in the right-hand panel of figure 15 which shows no saturation phenomenon in the dependence of the characteristic temperatures on  $\Upsilon$  for the helix. Instead, both  $T_{\text{min}}$  and  $T_f$  grow with  $\Upsilon$  except at small values of the parameter. However, the folding times and the distributions of the defects in chirality do saturate with  $\Upsilon$  around the value of 1, so from now on we consider the canonical case of  $\Upsilon = 1$ .

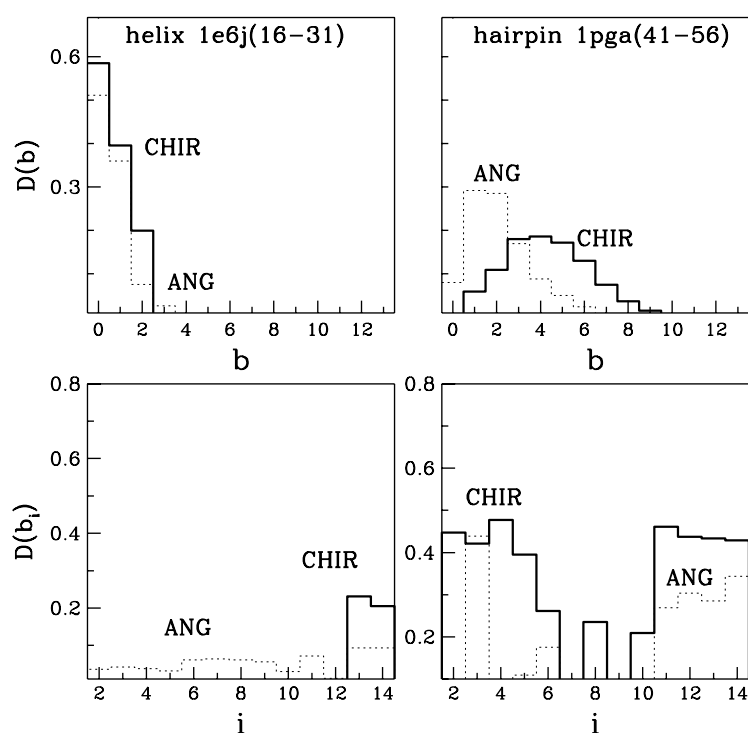
Figure 16 compares the distribution and localization of the defects in chirality obtained by incorporating  $V^{\text{CHIR}}$  to those with  $V^{\text{ANG}}$ . In both cases, the folding is declared by means of the  $Q$  criterion. It is seen that the angular terms perform about the same, or slightly better, in eliminating the defects in the helix (the defects with  $V^{\text{ANG}}$  are also found to be delocalized) but somewhat worse for the hairpin and crambin (not shown). In crambin,  $V^{\text{CHIR}}$  may yield up to 14 defects whereas  $V^{\text{ANG}}$  may yield up to 9. We find, however, that the computer time is significantly shorter when using  $V^{\text{CHIR}}$  than when using  $V^{\text{ANG}}$  because of the difference in effort taken to calculate the potentials and to derive forces. Thus  $V^{\text{CHIR}}$  appears to generate about the same conformational effect as  $V^{\text{ANG}}$  but the calculations proceed faster. A purist's approach would be to include both terms in the Hamiltonian.

## 6. The side groups

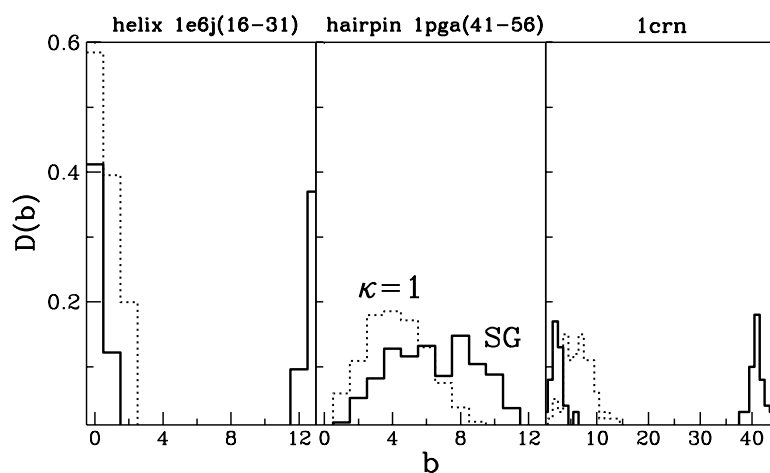
The origin of chirality effects in proteins sits in the atomic structure of amino acids. Suppose we generalize our Go-like model so that it includes the  $C^{\beta}$  atoms in addition to the  $C^{\alpha}$  of the backbone. Our version of this generalization will be described in a separate publication and it involves interactions between two kinds of effective atoms representing particular amino acids. The extra degrees of freedom generate a more sophisticated set of steric constraints. Will these constraints be sufficient to account for the chiral effects?

Figure 17 suggests that such a modelling of the side groups in itself does not guarantee emergence of the correct chirality when the native contacts are established and, in fact, fares worse than the simple Go-like model with the chirality term. The side group modelling based on the  $C^{\beta}$  atoms still requires augmentation with the chirality potential. We note that the chirality defects in the side group model are found to be delocalized.

We conclude that the chirality potential with  $\kappa$  equal to 1 or larger is a useful and important ingredient of Go-like models of proteins. The chirality-related criteria of folding should also be of value when considering models that go beyond the Go approximation. Our results



**Figure 16.** The same as figure 3, but with the chiral potential (solid line) or with the angular potential (dotted line) added to the contact interactions and the tethering terms. Folding is decided on the basis of the  $Q$  criterion.



**Figure 17.** The distribution of the wrong signed chiralities for the systems indicated and modelled by the Go-like Hamiltonian with the side groups (SG—the solid lines) and by the Go-like Hamiltonian without the side groups but with the chirality potential corresponding to  $\kappa = 1$  (the dotted line). The  $Q$  criterion is used here to determine folding.

were illustrated for two specific examples of secondary structures and one protein. However, similar results were found for several other helices (1fv(127–142) and 1f63(3–18)), another

Ipga hairpin and two other proteins: 1rpo and 1efn. We have found that the  $\alpha$ -protein 1rpo behaves like a helix in that it responds correctly to the chirality potential better than to the angular potential.

### Acknowledgments

We acknowledge support from KBN in Poland (grant number 2 P03B 025 13) and thank A Kolinski for letting us use his computer cluster.

### References

- [1] Li M S and Cieplak M 1999 *J. Phys. A: Math. Gen.* **32** 5577
- [2] Li M S and Cieplak M 1999 *Phys. Rev. E* **59** 970
- [3] Hoang T X and Cieplak M 2000 *J. Chem. Phys.* **112** 6851
- [4] Hoang T X and Cieplak M 2001 *J. Chem. Phys.* **113** 8319
- [5] Abe H and Go N 1981 *Biopolymers* **20** 1013
- [6] Takada S 1999 *Proc. Natl Acad. Sci. USA* **96** 11698
- [7] Ortiz A R, Kolinski A and Skolnick J 1998 *Proteins* **30** 287
- [8] Cieplak M and Hoang T X 2003 *Biophys. J.* **84** 475
- [9] Bernstein F C, Koetzle T F, Williams G J B, Meyer E F Jr, Brice M D, Rodgers J R, Kennard O, Shimanouchi T and Tasumi M 1997 *J. Mol. Biol.* **112** 535
- [10] Cieplak M and Hoang T X 2002 *Int. J. Mod. Phys. C* **13** 1231
- [11] Tsai J, Taylor R, Chothia C and Gerstein M 1999 *J. Mol. Biol.* **290** 253
- [12] Veitshans T, Klimov D and Thirumalai D 1997 *Folding Des.* **2** 1
- [13] Betancourt M R and Skolnick J 2001 *J. Comput. Chem.* **22** 339–53
- [14] Cieplak M 2004 *Phys. Rev. E* **69** 031907
- [15] Chen Y, Zhang Q and Ding J 2004 *J. Chem. Phys.* **120** 3467
- [16] Kolinski A, Jaroszewski L, Rotkiewicz P and Skolnick J 1998 *J. Phys. Chem. B* **102** 4628–37
- [17] Boniecki M, Rotkiewicz P, Skolnick J and Kolinski A 2003 *J. Comput. Aided Mol. Des.* **17** 725–37
- [18] Clementi C, Nymeyer H and Onuchic J N 2000 *J. Mol. Biol.* **298** 937–53
- [19] Cieplak M and Hoang T X 2003 *Physica A* **330** 195